The Journal of Experimental Biology 208, 3145-3158
Published by The Company of Biologists 2005
doi:10.1242/jeb.01753

Geometry of elytra opening and closing in some beetles (Coleoptera, Polyphaga)

Leonid Frantsevich[1,2,*], Zhendong Dai[2], Wei Ying Wang[2] and Yafeng Zhang[2]

[1]*Schmalhausen-Institute of Zoology, 15 B. Khmelnitsky Str., Kiev 30, 01601, Ukraine* and [2]*Nanjing University of Aeronautics and Astronautics, 29 Yudao Street, Nanjing, Jiangsu 210016, China*

*Author for correspondence (e-mail: leopup@izan.kiev.ua)

Accepted 14 June 2005

Summary

Elytra in beetles move actively, driven by their own muscles, only during transient opening and closing. The kinematics of these movements have been inadequately described, sometimes controversially. Our goal was a quantitative 3-D description of diverse active movements of the elytra, in terms of directions of the axes of elytra rotation.

Broad opening and closing was video recorded in beetles, tethered by the mesothorax, and has been analyzed frame by frame. For tracing, small dots or straw arms were glued to the elytra. Opening and closing traces coincided. The trace of the elytron apex was a flat circular arc about the axis of abduction–adduction (AAA). The rising hemiaxis pointed contralaterad. The AAA was tilted forwards in *Melolontha hippocastani*, *Allomyrina dichotoma* and *Prionus coriarius* but backwards in *Chalcophora mariana*. In *Cetonia aurata*, the AAA had a low elevation and a strong backward orientation. If another elytra-fixed point was traced in addition to the apex (in *M. hippocastani* and *P. coriarius*), then secondary rotation about the sutural edge (supination on opening) occurred. Modeling of abduction–adduction revealed that the elytron rose on opening if the AAA pointed contralaterad. The more the AAA was tilted forward, the more negative was the attack angle of the open elytra. The negative attack angle was partly compensated by positive body pitch and, more effectively, by supination of the costal edge about the sutural edge.

The initial stage of opening included elevation of closed elytra (by 10–12°) and partition to the sides, combined with an inward turn (<2–3°). Axis of rotation at this stage presumably coincided with the AAA. Movement of one elytron with respect to the opposite one at the beginning of opening followed the shallow arc convex down. The geometry of this relative movement describes the initial partition of the elytra and release of the sutural lock.

Key words: biomechanics, coadapted structure, Coleoptera, Polyphaga, elytra, elytral lock, insect flight.

Introduction

Wing-to-body articulation in insects is by a complex kinematic chain of several sclerites. It has three degrees of freedom: the wing flaps up and down and, in addition, forwards and backwards relative to the trunk; on transition between these phases, the moving wing blade flips (supinates) or flings (pronates) about its longitudinal axis. By opening from the rest position to the flight position, the wing spreads out (abducts) and, in certain insect orders, unfolds. The reverse adduction occurs on closing into the rest state (reviewed by Brodsky, 1994). Beetles have evolved complicated kinematics of wing unfolding (Schneider, 1978; Haas and Beutel, 2001).

The elytra in beetles are the forewings, modified for a protective function. The rigid elytra reliably seal the wings and abdominal spiracles inside the subelytral space. This adaptation allows beetles to penetrate soil, bark, wood and water, an enriched diversity of ecological niches, and facilitates enormous adaptive radiation. Sealing is provided by many locks between the perimeter of the elytra and the body, between the elytra and the underlying wings and between the two elytra themselves (down their anal edges) or by the suture (see details and references in Discussion).

Physiological study of elytral movement is hindered by the covert position of the mesothorax in beetles: for example, of the whole mesotergite, only the scutellum is exposed. Suggestions on the role of mesothoracical muscles were derived from anatomical observations on separate muscles, without understanding their action in concert.

Mobility of the elytra is simple compared with that of the hind wings. Indirect fibrillar muscles, which drive the wings, are absent from the mesothorax. If elytra do beat in synchrony with wings during flight, they do so passively due to mechanical coupling between the meta- and mesothorax (Schneider and Meurer, 1975). Autonomous movements of elytra only occur during transitory opening and closing, driven by a limited set of direct and indirect elytral muscles.

There exist several anatomical descriptions of how the elytra open and close (see details in Discussion), and these descriptions are sometimes contradictory. Previous cine

recordings of elytra, together with wings, during flight (Schneider, 1986, 1987; Schneider and Hermes, 1976; Schneider and Krämer, 1974) did not include the transient opening and closing. The first goal of our study was to film this transient process and to derive a quantitative three-dimensional (3-D) description of opening and closing relative to the elytra-bearing segment, the mesothorax. We aimed to answer the following questions: (1) are there distinct stages during opening (closing); (2) how diverse are the movements of the elytra and (3) how is the axis (or axes) of elytra rotation directed? The 3-D description gives a basis for further quantitative understanding of the complicated kinematics of elytra-to-body articulation.

Our final goal was to elucidate the relative partition of the two elytra on opening (or the reverse on closing). This problem is regarded with respect to the sutural lock: this lock is released by the simultaneous motion of two elytra relative to each other, while all other locks are released by movement of the given elytron relative to the body. Relative motion of two rotating bodies creates peculiar geometry. For example, elaborate shapes of the teeth in gear wheels have been constructed taking into account similar relative movement of wheels. If parts of a lock are pulled in a particular direction on opening, then the lock must provide easy partition in this very direction but must block other imposed forces. Our question is whether the shape of the relative partition on opening influences the shape of the sutural lock.

We present data on 3-D measurements of opening and closing of the elytra in large beetles that belong to Schneider's *Cantharis* and *Oryctes* types (Schneider, 1978).

Materials and methods

Insects

Insects (Lucanidae – *Serrognathus titanus* Bsd.; Scarabaeidae – *Melolontha melolontha* L., *Melolontha hippocastani* F. (Melolonthinae), *Catharsius molossus* L. (Scarabaeinae), *Allomyrina dichotoma* L. (Dynastinae), *Cetonia aurata* L., *Liocola brevitarsis* Lewis (Cetoniinae); Buprestidae – *Chalcophora mariana* L.; Cerambycidae – *Prionus coriarius* L.) were caught in the field. For the morphological analysis, we used dry specimens of other species from collections. Sections across the sutural area of the separated elytron were cut by hand with a sharp razor blade; elytra were macerated in 10% NaOH for different periods of time (0.5–3 days) before sectioning.

Videorecordings

In preliminary observations, beetles were tethered from above at the pronotum. Later, they were tethered from below at the meso- and metasternum to a wire holder (2 mm diameter) with cyanoacrylate glue. Cock-chafers, *Melolontha*, were tethered at the lateral surface of the meso- and metapleura. Legs were clipped, to prevent grasping. The beetle was mounted straightly, at an approximately horizontal body orientation, or tilted head up by 20–40°. A mirror, inclined by 45°, was placed above the beetle. Beetles were stimulated to fly by blowing an air stream from a fan.

Small paper marks with black dots were glued onto the tips of the elytra. In other experiments, we prepared light tripods of three 15 mm pieces of thin straw, glued together at right angles. Each tripod weighed 28–34 mg. One tripod was glued to each elytron. Black dots or tips of tripods are referred to below as 'landmarks'. A tilted body orientation was used in order to obtain better views of the landmarks both in the real and mirror fields. The insect was viewed using a video camera from behind as a real image and from above as a mirror image. Scales of the real and mirror images were calibrated. The set-up was illuminated with a 300 W projector lamp.

A digital video camera recorder (Panasonic NV-A3EN, Matsushita Electric Industrial Co., Japan) was used for recordings at a frame rate of 25 frames s^{-1}. This rate was evidently below the wing stroke frequency. Due to bright illumination and a short exposure of 2 ms, we obtained sharp images of the elytra in various positions in repetitive episodes of opening and closing, enough to trace the trajectory of the landmark on the elytron. A series of episodes at the same body orientation comprised one film series. Selected episodes were digitized with the aid of a videocard ATI Rage Pro Furi Viva (ATI Technologies, Inc.) and the program ATI Video In 6.3 (ATI Technologies, Inc.), with further compression into the format DivX MPEG4 Fast motion.

Data processing

To track the motion of the elytra, we needed to obtain the 3-D positions of landmarks, which were obtained from the geometric position of marker points from each image in both real and mirror fields through frame-by-frame analysis. Two programs, AVIEdit (AM Software, Moscow, Russia) and Sigma Scan Pro (SPSS Inc., Chicago, IL, USA), were launched in parallel windows. Numbered frames, displayed by AVIEdit, were copied into the Sigma Scan image window, where relevant points were indicated and their pixel coordinates were saved as an Excel 5.0 (Microsoft Corporation, Redmond, WA, USA) table.

We used several coordinate systems for 3-D measurements and spatial transformations: the global system was fixed to the video camera or video frame, the second, body-fixed system was fixed to the beetle's mesothorax, and the third system, determined by the landmark, was fixed to the moving elytron. By modeling the movement of a flat elytron, we introduced the fourth system, fixed to this flat elytron. Definition of axes in the images, as well as definitions of other coordinate systems, are given in Table 1.

The frame contains the real and mirror images of the beetle. Each image is a projection of the beetle on two global axes (Fig. 1). In each image, we indicated either the apex of the scutellum and two marks on the elytra, or the scutellum and the arms of the tripod. The apex of the scutellum was adopted as the origin of the global coordinate system. After proper scaling of the real and mirror images, coordinates of relevant points were measured with respect to the scutellum. The real

Table 1. *Axes of coordinate systems used in this study*

System	Origin	Axis	Positive direction
Global, camera-fixed, real image	Hind corner of the scutellum	*x*	Horizontal, to the right
		y	Vertical, upwards
		z	Down the optical axis, to the head of the beetle, unobservable in the frame
Global, camera-fixed, mirror image	Hind corner of the scutellum	*x*	Horizontal, to the right
		y	Unobservable
		z	Vertical, to the head of the beetle
Body-fixed	Hind corner of the scutellum	*q*	Transverse, to the right
		p	Longitudinal, forward
		v	Dorsad
Landmark-fixed	Center of landmark rotation	*a*	Dorsal hemiaxis of landmark rotation
		w	Radius-vector from the center to the landmark
		b	Binormal, orthogonal to *a* and *w*.
Fixed to the flat model elytron	Elytron-to-body articulation, O	*t*	Down the basal edge of the elytron, laterad
		w	Down the sutural edge, caudad
		b	Binormal, orthogonal to *t* and *w*

image provided us with coordinates down the *x* and *y* axes, while the mirror image provided *x* and *z* coordinates.

Body-fixed axes have been defined approximately, without the use of prominent species-specific morphological markers. If the beetle is mounted straight, then the mesothorax-fixed transverse axis *q*, the longitudinal axis *p* and the vertical axis *v* correspond to the global axes *x*, *z* and *y*, respectively.

Further data processing for 3-D data presentation, analysis and modeling used Excel 2000, MatLab 6.5 (MathWorks, Inc., Natick, MA, USA) and custom programs written in Turbo Basic 1.3. The custom programs provided convenient tools for geometrical constructions in 3-D space. Graphic facilities were provided by Adobe Photoshop 5.5 (Adobe Systems, Inc., San Jose, CA, USA) and Corel Draw 5.0 (Corel Corp., Ottawa, Ontario, Canada).

Eleven film series were selected for digitization. They contained 139 episodes of opening and closing, totaling over 1850 frames. For each film, 3–16 dots were indicated in two images.

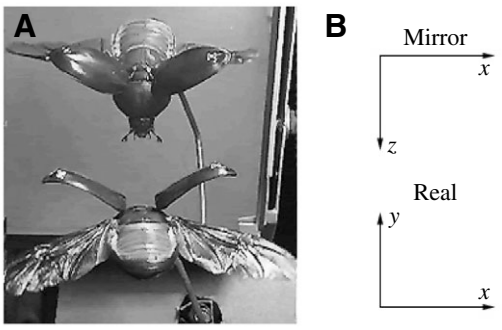

Fig. 1. The external reference frame. (A) Still frame of a tethered flying female of *Allomyrina dichotoma* at tilted body orientation. (B) Directions of coordinate axes of the external reference system in real and mirror images.

The error of localization of a certain dot in one image was 1–2 pixels (0.2–0.4 mm). The error accumulated during multiple spatial transformations. To assess the resultant error in the body-fixed reference frame, we measured the Euclidian distance, *D*, between tips of two arms in a tripod in four film series (445 frames). The standard deviation for *D* was in the range of ±0.35 to ±0.96 mm. We compared *D* with the coordinate of the longitudinal tripod arm tip down the axis of the camera lens. In three out of four records, regression of *D* on *p* (or *z* at tilted body orientation) was non-significant, meaning negligible perspective distortion.

The prime goal in data processing was to reveal planar rotation of the landmark. Hence, we neglected corrections for perspective and spherical distortions, because the plane transforms again into the plane after perspective transformations or in a skew coordinate system.

Results

Definitions

Only a few of the structures of the elytron are relevant to our study: (1) the sutural edge, (2) the costal edge, (3) the basal edge, (4) the apex at the distal tip of the sutural edge and (5) the root, the articulatory structure inserted between the tergite and the pleurite, which cannot be seen from outside in the intact animal. The root is shifted laterad with respect to the medial body plane. The size of the root is small. Thus, we assume below that the elytron is suspended at a fixed point.

We shall denote the broad spread of the elytra to the side, forwards and upwards as abduction on opening, and the reverse motion as adduction on closing. Additional rotation of the moving elytron about the sutural edge, the costal edge turning dorsad, is referred to below as supination, and the reverse rotation is pronation.

A definition of coordinate systems used in this study is given

in Table 1. Localization of the landmarks is measured and illustrated directly from the frames in the global coordinate system (x, y, z) relative to the scutellum. This localization is recalculated into the body-fixed system (q, p, v), where we compute the position of the axis of abduction–adduction (AAA). Additional supination of the abducting elytron (or reverse pronation on adduction) is revealed with the aid of the tripod landmarks in the landmark-fixed system.

The direction of the rotation axis, as well as of any vector, was expressed as a triplet of cosine directions (projections of the unit vector onto coordinate axes) or, more explicitly, as a pair of angles: 'elevation' is the angle between the vector and the horizontal plane (external or body-fixed), positive upwards; 'azimuth' is the angle (positive homolaterad) between the longitudinal axis p and projection of the vector onto the horizontal plane. Cosine directions were used in all vector computations.

Flexibility of the beetle's body and firm tethering

Preliminary filming revealed that a stag beetle, *Serrognathus titanus*, tethered at the pronotum, was able to flex and extend its head and the mesothorax (together with posterior body parts), with respect to the prothorax, by 50° and 40°, respectively. The mesothorax, metathorax and abdomen bent down on opening and rose on closing. The same behavior, with a lower angular span, has been recorded in the dung beetle, *Catharsius molossus*, and in the rose chaffer, *Liocola brevitarsis*. The prothorax is not a reliable place for taking measurements of elytron position with respect to the articulation site, the mesothorax. We decided to fix the beetle to a holder at the metasternum, which is firmly fused with the mesosternum, or at the meso- and metapleura.

The mesothorax itself is not a solid structure: the tergite is compressed down or rises with respect to the pleura during flight, and the pleura are able to shift laterad or mesad. The range of movements is small, even in large beetles, compared with the size of the whole elytron. Thus, we assume below that the elytron has a fixed articulation point.

First approximation: broad abduction–adduction

Opening of elytra in the tethered beetle lasted 50–60 ms in *Chalcophora mariana*, 40–150 ms in *Prionus coriarius*, 150–190 ms in *Allomyrina dichotoma* and 200–450 ms in *Melolontha hippocastani*. Closing lasted longer: 60–80 ms, 120–200 ms, 400–600 ms and 300–600 ms, respectively. The specimen of *P. coriarius* with tripods opened and closed its elytra in 80–120 ms, and the specimen of *M. hippocastani* with tripods in 300–450 ms, which is within the range of beetles with unloaded elytra. Three specimens of *Cetonia aurata* (all with tripods) opened and closed elytra in 60–170 ms and 80–150 ms, respectively.

Traces of the dot landmark in the external reference system (x, y, z) during opening and closing of the elytra are illustrated for three species in Figs 2–4. The shape of the trace depends on the pitch of the beetle: for example, traces are seen as arcs

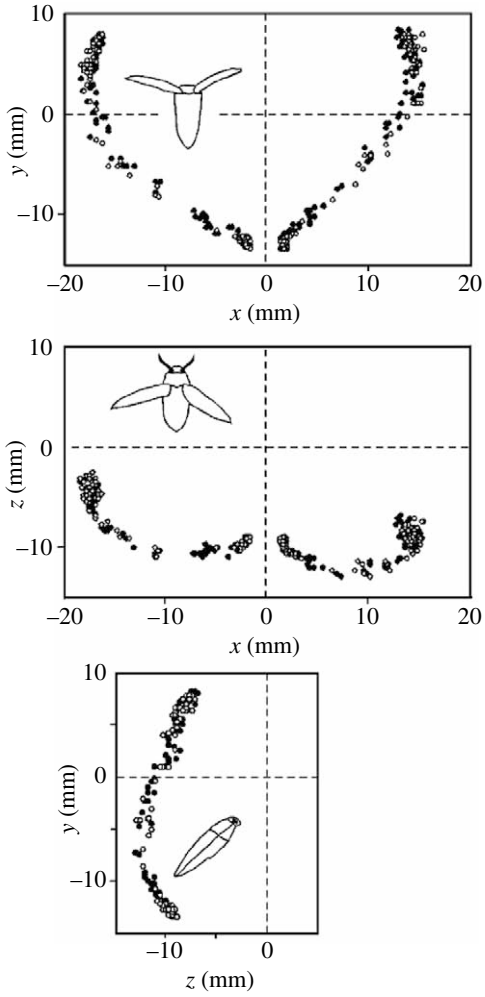

Fig. 2. Traces of the landmark dots on the elytra in *Chalcophora mariana* shown as three projections in the external reference system during opening (open dots) and closing (filled dots). Locked positions are near the zero x value. Traces coincide on their opening and closing courses. Pitch 47°, 33 episodes, 195 frames. Body silhouettes in the top (real image) and middle (mirror image) panels are drawn from still frames, while the silhouette in the bottom (reconstructed) panel is shown with closed elytra.

in the jewel-beetle, *C. mariana*, tethered at a skew (Fig. 2). The trace in the sagittal plane was reconstructed and appeared to be least informative. The traces of opening and closing overlay each other almost perfectly, especially at the smaller angles of turn. If two curves coincide in two projections, they coincide in 3-D space. Below, we process both traces together.

In a cock-chafer, *M. hippocastani* (Fig. 3), and a long-horn beetle, *P. coriarius* (Fig. 4), both mounted at a skew, we observed traces that looked like straight segments in the projective plane x–y. In the jewel-beetle, on the other hand, the straight trace in this projection was seen at the straight body orientation of the insect. It is possible to rotate traces in 3-D space so as to see one of them stretched down a straight line or to see both as arcs (Fig. 5).

We noted that traces sometimes contained additional parts

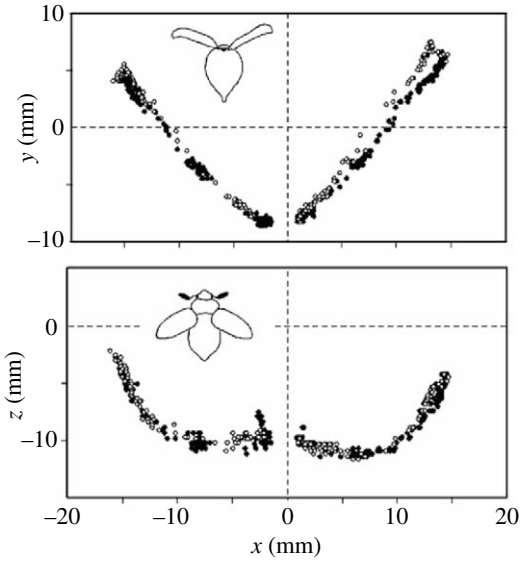

Fig. 3. Traces of landmark dots on the elytra in *Melolontha hippocastani* in two projections in the external reference system during opening and closing. For designations, see Fig. 2. Pitch 35°, 7 episodes, 354 frames.

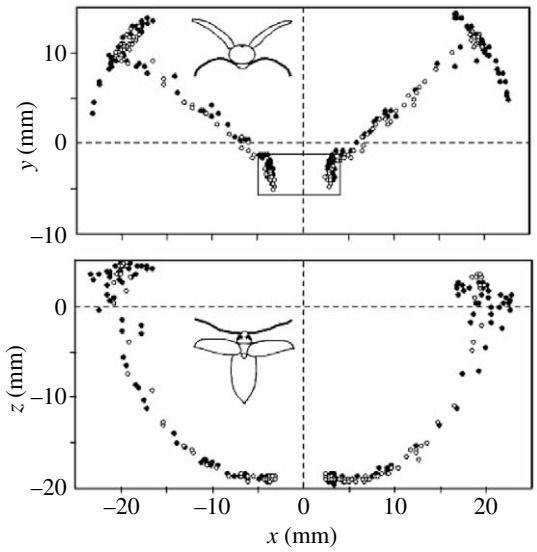

Fig. 4. Traces of landmark dots on the elytra in *Prionus coriarius* in two projections in the external reference system during opening and closing. Top panel: rear view in the real image, bottom panel: top view in the mirror. For designations see Fig. 2. Note (i) parallel rising at the start of opening and sinking down at the finish of closing (box in the top panel) and (ii) traces of wingbeats of the elytra after opening and before closing seen as mushroom heads in both panels. Zero pitch, 9 episodes, 157 frames.

directed across the main trace of opening–closing in the completely open position of the elytron. It is most explicitly seen in Fig. 4. We can explain the origin of this appendix by capturing some wingbeat frames. Schneider and Krämer (1974) and Schneider and Meurer (1975) stated earlier that wingbeats of elytra differed in direction from opening and

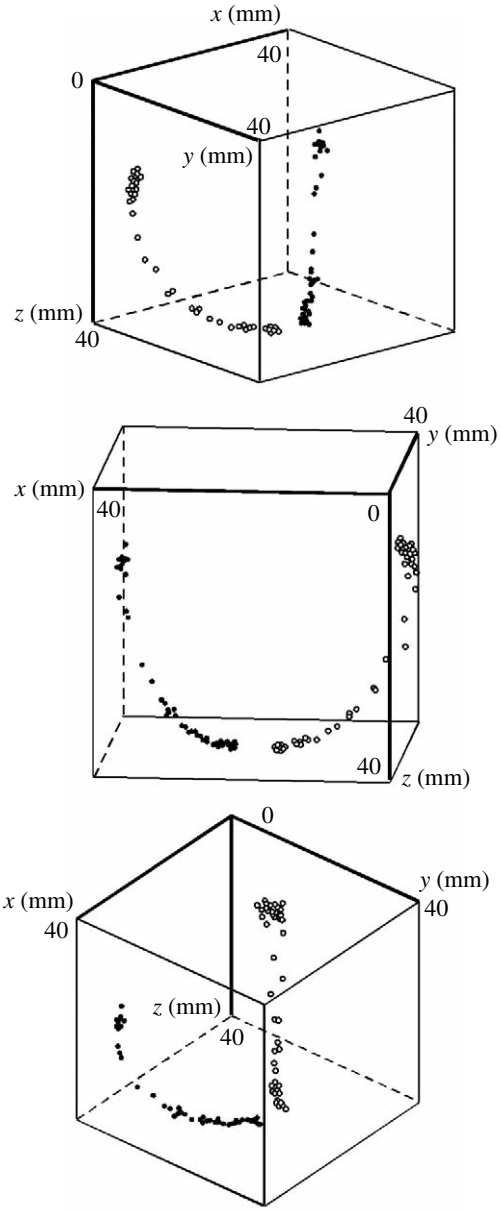

Fig. 5. Traces of landmark dots on the opening elytra of *Prionus coriarius*, subtended at different aspects in the external reference system. Open dots, left elytron; filled dots, right elytron. The side of the cube is 40 mm, bold ribs converge at the point (+20, +20, +20 mm). The 3-D graph can be tilted so that dots lie approximately along a straight line on either trajectory, or both trajectories are seen as arcs.

closing. We do not consider the wingbeats of the elytra in the present article.

The radius-vector from the articulation point to the landmark is obviously constant. During arbitrary rotations of the elytron, this radius-vector, as the generatrix of a cone, circumscribes a conical surface. The trace of the end-point is the ‘base’ of the cone in 3-D space, but is not necessary flat. If a trace has a straight projection at a certain view, then this trace lies within a plane. Hence, the flat base of the cone with the generatrix of constant length is the flat arc of a circle.

Table 2. *Mean direction of the axis of abduction–adduction in beetles*

Species	Episodes (frames)	Direction (deg.)		Mean vector	Angles (deg.)*	
		Azimuth	Elevation		Right to left	Turn
Melolontha hippocastani	36 (873)	–78.8	44.4	0.9074	79±14	76±7
Prionus coriarius	26 (423)	–80.1	41.3	0.9930	96±14	97±6
Chalcophora mariana	26 (180)	–135.3	60.4	0.9929	40.7	80.2
Allomyrina dichotoma	4 (75)	–64.3	30.5	0.9911	101.8	94.3
Cetonia aurata	8 (16)	–153.3	17.3	0.9748	117.2	12.2

*Values are means ± S.D.

Fitting of a circle to the random cloud of 3-D dots is a puzzle, because five parameters are unknown: the three coordinates of the center and the two angles, which characterize the tilt of the base plane. Having only a short arc of the circle, we applied an heuristic solution: mark three dots at the beginning, in the middle and at the end of the arc and construct a plane and then a circle across these dots in 3-D space. Computation returns the position of the center, the radius, the arc of the turn and the direction of the normal to the plane of the circle. The direction of the normal coincides with the direction of the rotation axis. We conventionally call this the 'axis of abduction-adduction' (AAA). Below, we apply the name 'radius-vector' only to the line between the center of the circle (not coinciding with the articulation point!) and the dot landmark. The quality of this approximation is verified in the section below on relative multiple rotations.

We applied the same procedure to the tip of the longitudinal tripod arm as the landmark for the wing apex. In two film series, we constructed circles by three selected frames in separate episodes, with further averaging of axial vectors.

For the insects mounted straight, the direction of the AAA in the external and body-fixed reference systems coincides. For insects filmed at tilted body orientation, we used the coordinate transformation according to the body pitch. Then we changed the sign of the *q*-component for the left elytron and averaged the axis directions for both elytra as 3-D unit vectors. Mean direction refers to the right side. All data are pooled together in Table 2.

Despite the large scatter of data, due to the difficulty of controlling the symmetry of mounting and landmarking, pixelization errors, cumulated errors of spatial transformations, the rough method of circle construction, and the eventual asymmetry in elytra performance, we noticed some general features in the organization of the AAA.

The rising half of the AAA always pointed contralaterad (positive *v*-component, negative *q*-component). In *M. hippocastani*, *A. dichotoma* and *P. coriarius*, the AAA was tilted forwards (positive *p*-component). Indeed, we have observed straight traces of the landmark, when the beetles had positive pitch and the AAA occurred in the image plane. By tilting the beetle head down to zero pitch, we tilt the AAA forward. The AAA pointed backwards in the jewel-beetle, *C. mariana*. The angle between the right and left AAA was assessed in the approximate range of 40–110°, while the angle of turn about the AAA was assessed in the range of 75–100°.

The main conclusion is that the apex of the elytron rotates flatly during opening and closing. The method of construction of the AAA is explained in the Appendix.

Initial stage of opening

Opening is preceded by a downward movement of the abdomen (probably together with the metathorax) and elevation of the still closed elytra. The inverse process has been observed at the end of closing. The trajectory of elevation-depression in *P. coriarius*, traced for the dot landmark, is illustrated in Fig. 4 (dots enclosed inside a box). Assessing the amplitude of elevation-depression as 3–4 mm and the distance from the articulation to the landmark as 18 mm, we derive the angle of elevation-depression to be ~0.2 rad (10–12°). Elevation-depression of a similar angular range was recorded in *M. hippocastani*. The axis of elevation-depression lay in parallel to the transverse body axis *q*.

At the very beginning of opening, a narrow slit appeared between the elytra. This partition might persist without further broad opening. The angle between the elytra was estimated as 2–3°. As is shown in the section below on modeling of elytra opening, the width of the sutural lock is ~0.1–0.3 mm at a distance of 10–20 mm from the base of the wing in large beetles. That means that the angular partition of elytra released from the sutural lock is much less than 1°.

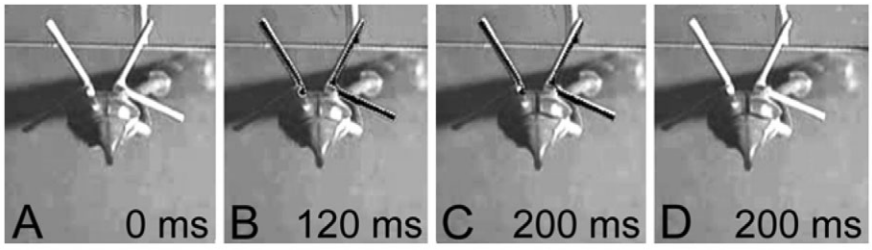

Fig. 6. Visualization of the small inward turn of elytra at the very beginning of opening in *Melolontha hippocastani*. Real images with tripods from still frames. (A) Initial closed position of elytra; (B) intermediate position; (C,D) final position of mini-opening. Negative images of white arms at the start position (now black) are overlaid onto B and C. Straight body orientation.

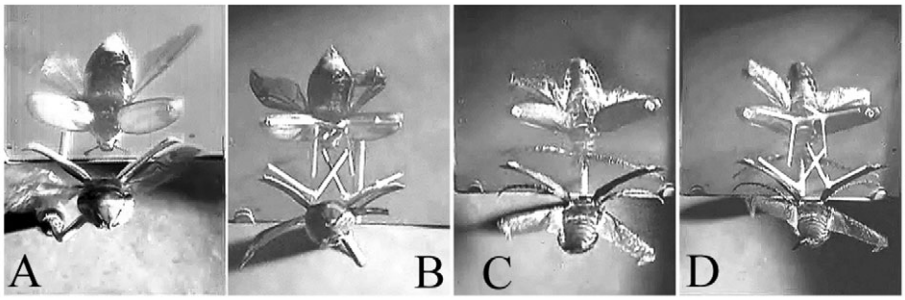

Fig. 7. Opening in tethered beetles with and without tripods. (A,B) *Melolontha hippocastani* (different specimens, pitch about zero); (C,D) *Prionus coriarius* (same specimen, pitch 21°). Still frames. Real image is below.

It was impossible to trace such tiny movements in serial frames by pixelization. Visible turns of the elytra were accentuated with the aid of tripods. Watching movies frame by frame, we noticed that, in *Melolontha*, *Prionus* and *Chalcophora*, elytra *turned inward* while parting. In order to reveal tiny movements, we used the graphic facilities of Adobe Photoshop. The white arms of the tripods in the closed position were selected and inverted into black negative elements of the image. Then they were imprinted at the same localization into subsequent frames. A small shift of the white arm was then noticeable relative to the position of the black bar, the latter indicating the starting position (Fig. 6).

Second approximation: trace of supination

We assume that the elytron is rigid and suffers neither deformation, which differs from the flexible hind wing. We have defined above only two points: the articulation point and the apical landmark. We need at least one additional point to describe the turn of the elytron, because the 3-D position of a solid body is defined by the location of three non-collinear arbitrary points in this body.

In some experiments, we glued two orthogonal tripods on the elytra. They moved together with the elytron. The beetles with and without tripods are compared in Fig. 7. The size, mass and, obviously, moment of inertia of the elytron are comparable to or less than those of the tripod. The mass/length ratio of the elytra is 10 mg/12 mm in *C. aurata*, 10 mg/17 mm in *M. hippocastani* and 26 mg/30 mm in *P. coriarius*. Nevertheless, tripods do not affect the flight position of the elytra (Fig. 7) or the time of abduction–adduction.

One tripod arm (arm P) was aligned with the suture and approximately with the body-fixed axis *p*. The transverse arm (arm Q) pointed to the side and slightly downwards, and the third arm (arm V) pointed approximately upwards and a bit laterad, following the slope of the elytron. Arms are additionally described as L for the left elytron and R for the right elytron.

We selected two film series of *M. hippocastani* and *P. coriarius* for detailed analysis. In these series, tripods on opening did not touch the mirror and did not collide with the opposite tripod. Only two arms were traced for each elytron, because the third arm was obscured by the elytron in some frames. The tilted body orientation was better for recordings with tripods, because it provided more space for the elytra below the mirror. We describe frames recorded at the tilted orientation in the global coordinate system.

Tracing of arm P gave essentially the same results as tracing of the apical landmark; when the beetle was viewed from behind, straight traces were seen (Figs 8, 9B, traces LP and RP). This arm tip rotated flatly about the AAA. The direction of the AAA and localization of the rotation center (which did not coincide with the articulation point!) were derived from three arbitrarily selected points on the trace, as before. Parameters for the two elytra are stated in Table 3.

To check the quality of our reconstruction, we projected each point of the trace onto the axis of rotation and plotted the distance of the projection point from the center *versus* the angle of turn (Fig. 10). During flat rotation, this distance must be zero. We obtained the distances of 0.31±1.58 mm (mean ± S.D.) for the arm RP and 0.73±1.60 mm for the arm LP in *P. coriarius* and –0.44±0.88 mm for the arm RP and –0.62±0.96 mm for the arm LP in *M. hippocastani*. The displacement from zero and the scatter of points were small enough for reliable comparison with traces obtained in other arms.

Should the elytron rotate only about the AAA, all points of the elytron, as well as all points of arms fixed at the elytron, must encircle arcs about the AAA in parallel planes. Viewing from behind, we should see a trace of another landmark in parallel with the straight trace of arm P. This was obviously not the case (Figs 8, 9B). By computing projections of these landmarks on the AAA, as above, we obtained a steady rise of

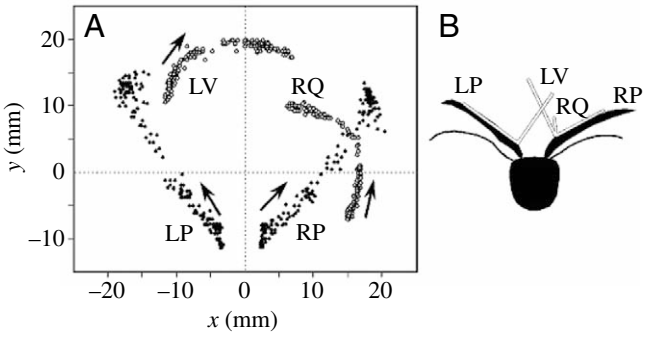

Fig. 8. (A) Traces of tripod arms in the real image plane in *Prionus coriarius* (rear view). (B) A silhouette of the beetle, drawn from a still frame, illustrates the positions of the tripod arms: LP, LV, arms of the left tripod; RP, RQ, arms of the right tripod; P, longitudinal arm; Q, transverse arm; V, vertical arm. Arrows indicate movement direction on opening. Rear view, pitch 21°, 13 episodes, 184 and 177 frames for two tripods.

the side landmarks Q or V *versus* turn angle in the right elytron for both beetles (Fig. 10). The rise of the costal edge indicated supination of the elytron on opening or reverse pronation on closing, because traces of opening and closing coincided for all tripod arms. The same suggestion about supination was derived from the traces of the left arms. Opening and closing of the whole elytron was not a simple rotation about the single axis: the elytron abducts about one axis and, at the same time, supinates about the other axis. The same holds true for adduction and pronation on closing.

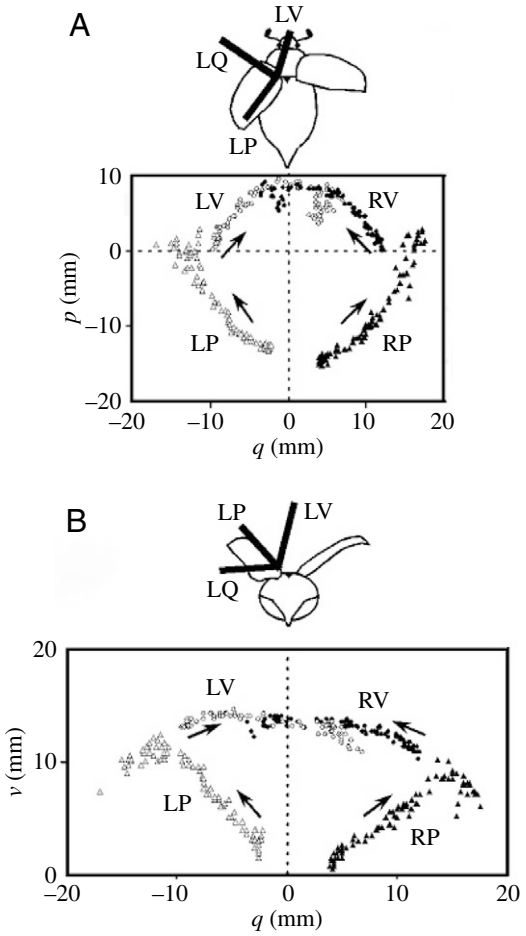

Fig. 9. Traces of tripod arms in the body-fixed reference system in *Melolontha hippocastani*. (A) Top view; (B) rear view. Body silhouettes at the top of each panel illustrate positions of the left tripod arms, clearly seen at the half-opened stage. Designations as in Fig. 8. Zero pitch, 4 episodes, 90 and 94 frames for two tripods. Note the elevation of elytra in the closed position (arms LP and RP in B) and the capture of wingbeats in the open position (arms LP, LV in A).

Relative multiple rotations

We defined the spatial position of the elytron by the articulation point and two landmarks. One may argue that our

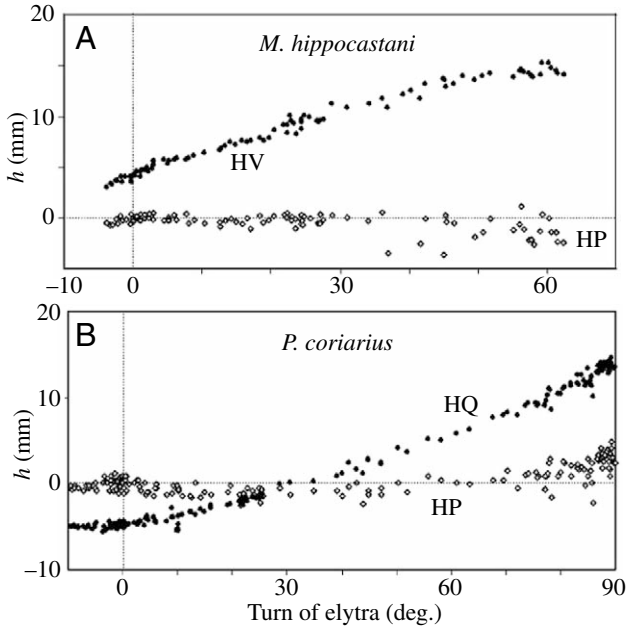

Fig. 10. Projections of two right tripod arm tips (P and either V or Q) on the axis of abduction–adduction in *Melolontha hippocastani* (A) and *Prionus coriarius* (B). Abscissa shows turn of elytra, in degrees, while the ordinate shows values in mm, positive upwards. HP, HQ, HV, location of projections relative to the center of rotation. Small scatter about zero for the arm P confirms proper reconstruction of flat rotation of this arm; trends in arms Q or V indicate additional supination.

Table 3. *Axes of rotation of two landmarks (tripod arms) on the elytra in the external reference system*

		Cosine directions on axes				
Species	Arm	*q* or *x*	*p* or *z*	*v* or *y*	Radius (mm)	Arc (deg.)
Melolontha hippocastani (zero pitch)	LP	0.8223	0.4624	0.3317	15.1	88.0
	LV	0.2400	–0.2941	0.9251	9.76	129.3
	RP	–0.6062	0.0550	0.7934	21.1	66.2
	RV	–0.0930	–0.5029	0.8593	12.58	82.9
Prionus coriarius (pitch 21°)	LP	0.8472	0.0120	0.5312	20.2	93.6
	LV	0.5177	–0.7953	0.3153	15.6	88.0
	RP	–0.7733	0.1850	0.6065	18.8	85.8
	RQ	–0.5680	–0.7463	0.3469	13.6	106.9

LP, LV, arms of the left tripod; RP, RV, RQ, arms of the right tripod.

landmarks were placed arbitrarily. Even the apex is an arbitrary point, convenient for tracing. Tripod arms increase the radius of rotation and facilitate measurements.

Hence, the direction of the elytral rotation may be defined only with respect to the elytron-fixed landmark. In general, any landmark on the elytron might be set for description of the primary, body-fixed movement. In order to investigate this problem, we analyzed movement of the left elytron in *M. hippocastani*, because it showed the best unbiased coordinate transform (S.D. of the interarm distance was ±0.35 mm; correlation between the interarm distance and the distance from the camera was 0.14).

For both landmarks, P and V, we constructed circles of their body-fixed flat rotations. Now, we introduce a new reference frame: fixed to the landmark (Table 1). Three axes, *a*, *w* and *b*, comprise a local basis of the elytron, which in turn moves in the body-fixed space. If we select the landmark P as the primary one, then projection of this landmark on the axis *a* is scattered about zero (Table 4). Projection on the axis *w* is scattered about the mean radius of rotation, with small standard deviations. Projection on the binormal axis (*b*) equals zero. By contrast, the trace of the other landmark, V, within the arm P-fixed system, shows great scatter in projections on the three mentioned axes.

We obtain similar results by selecting arm V as the primary landmark and checking the quality of construction of the body-fixed circle of rotation. Precision is worse here due to the smaller radius; however, standard deviations are of the order of 1 mm. Another landmark, now P, shows larger scatter. The axis of rotation of the landmark V is tilted backwards (negative *p*-component) in the body-fixed system and lies close to the body vertical (Table 3). Angles between two axes – one for the longitudinal arm landmark and the other for the side arm – lie in the range of 57–68° in both beetle species.

By computing traces of two arms in two arm-fixed systems (Fig. 11), we observed less dot scatter for the primary landmark about the position of the radius and more-or-less broad arcs for the secondary landmark. This feature was better reconstructed for the arm P-fixed system. The trace of side arm V, viewed from the tip of the arm P, rotated clockwise about the longitudinal wing axis on opening; that means supination of the costal edge for the left elytron. The direction of the 3-D turn of arm P in the V-fixed system was hard to interpret in anatomically reasonable terms.

Table 4. *Statistical parameters of landmark (tripod arms) projections of the left elytron in* Melolontha hippocastani *onto arm-fixed systems (90 frames)*

System fixed to arm	Arm	Projection on the fixed axes (mm)*		
		Axis *a*	Axis *w*	Axis *b*
P	P	–0.62±0.96	14.89±0.43	0
P	V	12.33±5.33	7.75±2.19	7.24±7.52
V	V	0.50±0.81	8.96±1.28	0
V	P	–2.42±1.38	–5.58±2.43	–11.29±2.12

*Values are means ± S.D.

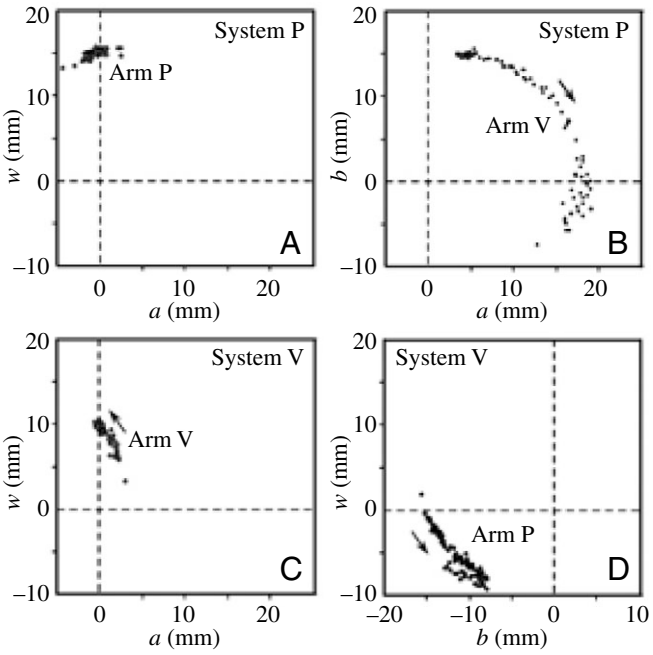

Fig. 11. Traces of two landmarks (tripod arms) in two arm-fixed coordinate systems, reconstructed for the left elytron in *Melolontha hippocastani*. (A,B) Traces of two arms in the arm P-fixed system; (C,D) Traces of two arms in the arm V-fixed system. A and C show traces of the referent arm in its own fixed system, while B and D show traces of another arm in the former system. The reference arm-fixed system rotates together with the elytron about the body-fixed axis, while the other arm turns about the radius-vector of the reference arm. Each arm may be set as the reference one. Zero pitch, 4 episodes, 90 frames.

Opening and closing in rose-chafers

Elytra movements in Cetoniinae are of small amplitude. Therefore, it was impossible to trace elytra-fixed points reliably in the short course of their rotations. At the first approximation, we applied the model of flat rotation of the whole elytron. We filmed the insect at straight mount, head to the camera, with the tripod on each elytron. We compared orientations of tripod arms (with respect to the apex of the tripod) for the elytron in its open and closed positions. Four films of opening and closing were analyzed, and a total of 288 dots was pixelized in 16 frames (including the scutellum). The check angle between the tripod arms was estimated as 90.26±2.35°, and arm length as 15.5±0.49 mm (mean ± S.D.). The distance between tripod tips diminished on opening by 0.74±0.09 mm (mean ± mean error), which is significantly different from zero according to the Student's *t*-test (P_0<0.1). That meant some perspective distortion.

For each of eight episodes of opening or closing, we fitted three unknown parameters (azimuth and elevation of the rotation axis and arc of turn) with the aid of an interactive iterative program, which started from the open position of the

Table 5. *Statistical parameters of tripod rotation on opening and closing in* Cetonia aurata*: position of rotation axis (azimuth, inclination, cosine directions) and arc of turn*

	Fitted angles (deg.)*				Cosine directions on axes			
Tripod	Azimuth	Elevation	Arc	Error (mm)	*q*	*p*	*v*	Mean vector
Left	−146±8	25±3	14±2	0.98	0.4983	−0.7519	0.4316	0.9916
Right	−160±7	9±4	11±2	0.67	−0.3447	−0.9261	0.1530	0.9909

*Values are means ± S.D. (16 frames).

tripod and compared the mean-squared Euclidian distance between the computed and observed localization of the three arm tips at the closed position for each combination of parameters (least square approach). The criterion of quality was the minimal value of the mean-squared distance per one arm (referred to as 'error' in Table 5). This error contained some systemic component because the longitudinal arm tip was partly obscured in open position, especially in the left tripod. Results of fitting are reported in Table 5.

The scatter of fitted values was rather tight for each tripod. The difference between the left and right tripods was due to the imperfect (non-symmetrical) mounting of the animal. Mean values are included in Table 2. A peculiar feature in *Cetonia* is the lowest elevation and strong backward pointing of the rotation axis, in addition to a small arc of rotation.

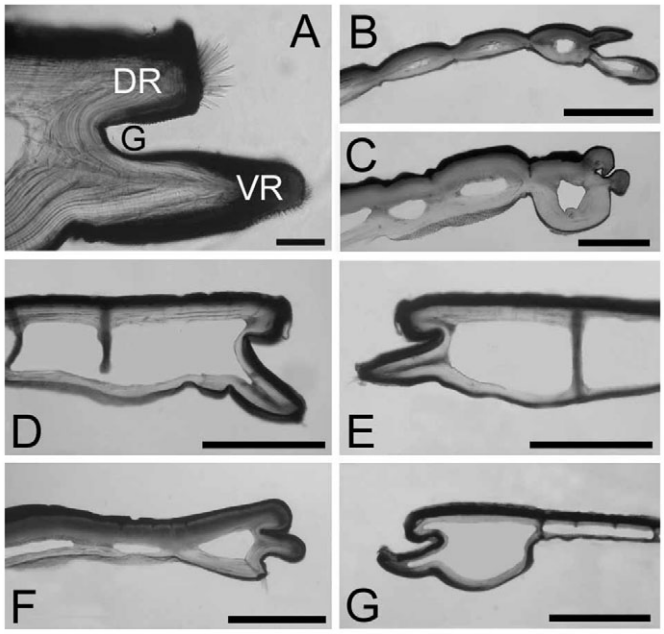

Fig. 12. Profiles of the sutural structures in some beetles. (A) *Catharsius molossus* L. (Scarabaeidae, Coprinae); (B) *Calosoma maximoviczi* Morawitz (Carabidae); (C) *Carabus elysii* Thompson (Carabidae); (D,E) *Allomyrina dichotoma* L. (Scarabaeidae, Dynastinae); (F) *Chalcophora japonica* Gory (Buprestidae); (G) *Rhomborhina unicolor* Motschulsky (Scarabaeidae,Cetoniinae). DR, dorsal ridge; VR, ventral ridge; G, groove. A, B and D show the female parts of the lock; the rest are male parts. Scale in A, 100 μm; B–G, 500 μm.

Profiles of the sutural lock

The narrow sutural face of the elytron consists of two ridges – the dorsal DR and the ventral VR – and the groove, G, between them (Fig. 12A). The dorsal ridge is short. Two opposite dorsal ridges meet together like stops in closed elytra. The ventral ridge of one elytron enters into the groove of the opposite elytron, like a blade into its sheath, and locks both elytra together. The groove above the blade is compressed into a narrow slit. The lock is made by a kind of 'male–female' plug. The temporary lock in winged beetles consists of an elongated blade and elongated groove of triangular or rounded profile (Fig. 12A,B,D–F). The blade in separated elytra is usually pointed horizontally or somewhat downwards. In a rose-chafer, *Rhomborhina unicolor*, we found that the profile of the blade was upwardly curved (Fig. 12G). The permanent lock in a wingless carabid, *Carabus elysii*, consisted of a short bulbous blade that fitted into the rounded groove of the opposite elytron (Fig. 12C).

The width of the dorsal ridge in temporary locks increased with the distance from the base of the elytron. At a distance of 15–20 mm from the scutellum, the depth of the groove did not exceed 0.2–0.3 mm.

Modeling of elytra opening

We modeled only flat elytra and typically limited their turns to 90°. We varied the orientation of the AAA to see how the orientation affected the final position. Fig. 13A–C illustrates the rotation of the elytron (horizontal at the start) *versus* the changing tilt of the AAA. Raising of the elytron is possible only if the AAA points contralaterad. The larger the azimuth, the steeper the rise of the elytron. If the AAA is tilted back (azimuth less than −135°), the attack angle after a turn by 90° may be positive, especially at high elevation of the rotation axis. If the AAA is tilted forwards (azimuth greater than −135°), the attack angle is negative. At an elevation of 45° and an azimuth of −135° or −90°, inclination of the elytron against the airstream is 8° or 45°, respectively, with a negative attack angle. At an azimuth of more than −90°, the final position of the elytron is even less streamlined.

We further analyzed behavior of the model (elevation 45°, azimuth −90°) with the elytra bent down at the start position. This posture is analogous to a beetle flying with positive pitch and observed from behind. The greater the bending (or higher the pitch), the more the elytron tended to horizontal placement

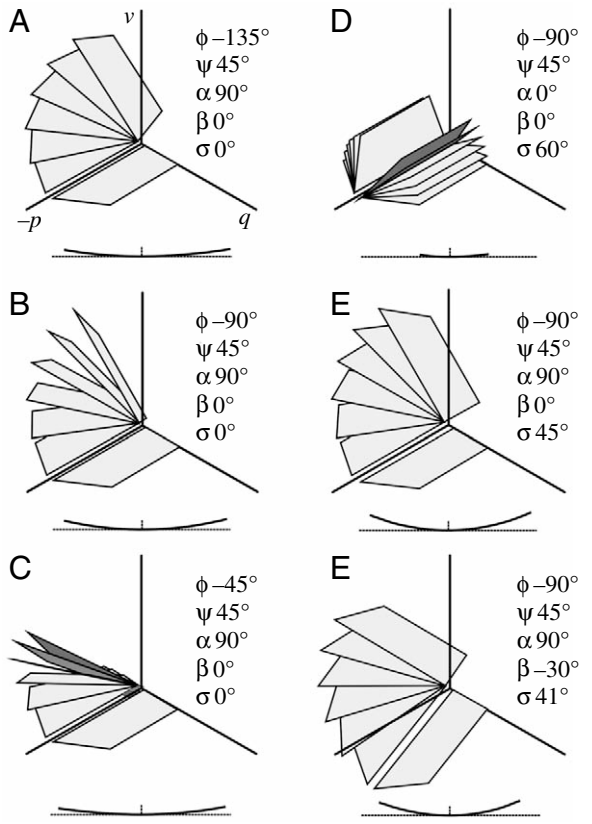

Fig. 13. Modeling of elytra motion. (A–C) Abduction of the left elytron by 90° *versus* different azimuth of the rotation axis (AAA). The smaller the azimuth, the more the open elytron tends towards a negative attack angle. (D–F) Supination combined with abduction; (D) supination of two elytra without abduction; (E,F) supinatory compensation of the attack angle to zero in the abducted left elytron. Initial position of elytra in A–E is horizontal, and in F is bent downwards. Angular variables are indicated in the panels: azimuth ϕ, elevation ψ, abduction α, bend β, supination σ. Isometric view in the body-fixed reference frame. Inset below each model, we show the trace of relative divergence in projection on elytron-fixed axes *t* and *b* (i.e. across the suture) upon initial abduction in the hypothetical range ±10°. The tracer moves to the left on opening. Trace in D is computed for parameters in *Cetonia aurata*.

(not illustrated). However, a bend of 45° improved the inclination of the elytron against the airstream only by 15° (from 45 to 30°). We conclude that flat rotation may not be enough to ensure an appropriate attack angle of the elytron during flight. It is impossible to put the elytron in a zero-resistance position without additional supination.

The model of secondary rotation about the straight sutural edge of the flat elytron is illustrated in Fig. 13D–F. The model allowed us to either supinate the elytral plane about the immobile sutural edge or to combine abduction and supination. It was possible to find, by iteration, the amount of supination that ensured horizontal placement of the elytron, i.e. minimal drag. Supination, consequently, improves the streamlined position against the airstream.

We also modeled the relative movement of the left elytron with respect to the right one at the beginning of opening. This model was computed in the right-elytron-fixed coordinate system (Table 1, final system). We computed abduction by 10° and also, hypothetically, rotation about the same AAA by −10° through crossed elytra, keeping in mind that the blade of the sutural lock penetrates into the opposite elytron. The trace of a point at the left suture relative to the right elytron is a shallow arc with positive curvature (convex down, the center of curvature is above the right elytron). This is illustrated in the insets in Fig. 13. Curvature is larger (or arcs are more convex) in models with additional supination. It is important to note that the curvature of the vault of the closed elytra is negative, opposite to the trace of divergence. Unlocking of the sutural lock must follow the surface of relative rotation.

Discussion

Opening and closing of elytra

Wing flap typically consists of two phases: the upstroke and the downstroke. The former is directed backwards in the beetles, the latter is directed forwards (fig. 34, item *12* in Brodsky, 1994). Supination and pronation of the wings during flight occur at transitory moments between the upstroke and downstroke (this may be the same for the flapping elytra). The wing rests on the dorsum and opens to the side, then backwards and upwards. The elytron opens (abducts) to the side, then forwards and upwards. Thus, it creates free space below for the wingbeats.

Movements of the elytra on opening and closing were examined long ago. Straus-Duerkheim (1828) named muscles in the cock-chafer, *Melolontha melolontha* L., according to their function. In particular, he discerned the direct flexor and extensor of the elytron (M35 and M42; *sensu* Larsén, 1966), the direct adductors (M36a, M36b) and the indirect adductor (M33). Further investigators described, not univocally, the turn of elytra on opening as a process of several stages. Functions of separate muscles will not be comprehensively discussed here.

Stellwaag (1914) distinguished unlocking, turn forward and then elevation in *Lucanus cervus* (Lucanidae). According to Herbst (1944, 1952), elytra in Melolonthinae, Rutelinae are initially opened slightly to the sides, and this is followed by the powerful elevation and outward motion. The elytra return (down) to their original position, driven by gravity and the elasticity of the mesonotum, whereas contraction of M36a closes them. According to the observations of Schneider and Meurer (1975) on *Oryctes boas* Fabr. (Scarabaeidae, Dynastinae), the elytra at the start flap forward, but only after release from their locks. The latter is possible if the elytra first rise at the sides. The forward turn is on a slant, because contraction of the direct M42 pulls the axilliary chain down and backwards. Belkaceme (1991) stated that the indirect M29 and M33 open the elytra by turning the scutellum forwards in *Noterus laevis* Sturm. (Noteridae). Reviewing the existing works, Matsuda (1970) concluded that elytra are extended simultaneously with elevation of the mesoscutellum by

cooperative contraction of M29 (t12) and M33 (t-p3), whereas M47 (t-tr1), which is lacking in scarabs, elevates the elytron. We conclude therefore that unlocking from manifold locks with the rest of the body is the generally accepted first stage, but further movements have only been conjectured. Some authors accept the notion of combined rotation on opening.

These earlier descriptions are far from the quantitative analysis that is required to gain a clear understanding of how the thoracical sclerites, direct and indirect muscles, multiple axilliary plates of complicated shape, and the blade of the elytron interact during opening and closing. Only Heberdey (1938) proposed a simple geometrical model of the rotation axis, which lay in the transverse body-fixed plane. Assuming that the transverse cross-section was an ellipse, the rotation axis connected the homolateral tip of the long, horizontal axis of the ellipse to the dorsal tip of the short axis. Hence, the rotation axis in Heberdey's model pointed contralaterad.

We have confirmed that elytra rotate about different axes during the initial elevation (final depression) of linked elytra, broad abduction–adduction and wing flaps. Such versatility is possible if the elytral articulation possesses three rotatory degrees of freedom.

Our measurements revealed that it is possible to describe the trajectory of the apex of the elytron on opening and closing as a flat rotation. Its axis lies at a skew and points contralaterad. Modeling of elytra opening confirmed that elevation of the elytron is possible only if the axis of rotation points contralaterad. This conclusion agrees with Heberdey's model, with the difference that the AAA, in general, is tilted forwards or backwards, in some taxa rather markedly (Cetoniinae).

Inspection of our model revealed that, after initially rising, the costal edge moves down. At least, after a turn of 90° or more, the elytron comes to the flight position with the negative attack angle, which may provide substantial drag. The situation is most marked in the case of forward inclination of the rotation axis, for example in the cock-chafer *M. hippocastani*, the rhinoceros beetle *A. dichotoma* and the long-horn beetle *P. coriarius.*

We found, further, that the positive body pitch partially compensated for the negative inclination of the elytra. Indeed, many beetles fly with positive pitch of the body. In particular, pitch was assessed in a cock-chafer by Nachtigall (1964). He calculated that passive lift of a dry specimen with 'naturally' opened elytra in the wind tunnel was maximal at a pitch of 27.5°. Brodsky (1988) cited even higher values for large beetles: 30° for a long-horn beetle (*Megopis* sp.), 40° for a rhinoceros beetle (*Strategus* sp.) and 60° for a jewel-beetle (*Julodis variolaris*).

Additional rotation is necessary in order to put the elytral plane in parallel to the opposite airstream. In our model, it was provided by supination of the elytral plane about the apical radius-vector. Indeed, the tripod technics revealed additional rotation of the moving elytron about the sutural edge, supination–pronation. Supination (pronation) is evenly distributed throughout the phase of abduction (adduction). We have demonstrated that both these rotations have only relative sense, with respect to the traced landmarks.

The standard and even abduction–supination on opening (or adduction–pronation on closing) suggests that the elytron moves as a mechanism with one degree of freedom and with one common drive. We believe that future studies will compare the 3-D organization of movements with the 3-D organization of pivots and hubs in the complex forewing articulation.

The diversity of beetles with respect to the geometry of the elytra, shapes of articulatory elements, set of driving muscles and flight posture must be taken into account. Observations of flying beetles revealed variability in open elytra positions among different species (Schneider, 1978), predominantly at a skew with respect to the vertical body axis. The extreme cases were almost horizontal orientation, in *Dytiscus marginatus* (Schneider, 1978) and histerids (Prasse, 1960; Frantsevich, 1981), and vertical placement, reported by Schneider (1978) in *Necrophorus humator* and *N. vespilloides* (Silphidae).

Locks to the body and unlocking

Breed and Ball (1909) first discovered the junction between the elytron and the rest of the body down the entire perimeter of the elytron. Stellwaag (1914) counted 14 kinds of locks, which we can classify as clamps, clicks and fields of microtrichia (Velcro™-type locks). Further investigations added several new locks to this list (Heberdey, 1938; Nachtigall, 1974; Nikolaev, 1987), especially when scanning electron microscopy resolved the variety in the fields of microtrichia underneath the elytron and thus contributed not only to understanding of their function (Gorb, 1998) but also to taxonomical differentiation (Baehr, 1980; Samuelson, 1996).

The strongest two locks are: (1) the clamp at the base of the elytron by the hind edge of the pronotum and (2) the subsutural click with the ridge on the metascutellum. These locks are released by the forward movement of the pronotum and depression of the metathorax (together with the abdomen) with respect to the mesothorax. Downward bending of the head, prothorax and abdomen was filmed during the unrestrained take-off of a leaf beetle, *Chalicoides aurata* (Chrysomelidae), by Brackenbury and Wang (1995). In *Pachnoda marginata* (Scarabaeidae, Cetoniinae), preparing for flight, the elytra and abdomen were separated by 5°. Elevation of the still-closed elytra before take-off was recorded also in a scarab, *Sisyphus schaefferi* (Prasse, 1960). These observations are completely confirmed by our own recordings on preliminary bending of the prothorax and the hind body with respect to the mesothorax and on elevation of the closed elytra before partition by 10–12°.

The inverse depression appears on closing, being complicated by the participation of vertical movements of the almost-closed elytra in order to fold the hind wings (Schneider, 1978; Haas and Beutel, 2001).

The sutural lock and unlocking

The sutural lock was noticed by early observers, Straus-

Duerkheim (1828) and Lacordaire (1834), described in more detail by Allaud (1902) and first depicted by Breed and Ball (1909). The lock is built by a kind of male–female plug. It is a matter of pure chance which ventral ridge – right or left – becomes the male component on eclosion (Pisano, 1982). Components of the sutural lock bear fasting areas, covered by short microtrichia or scales (Heberdey, 1938).

Any temporary lock performs two alternative tasks: to keep both components in tight contact against external disturbances and to release voluntarily with minimal effort. These contradictory demands are satisfied by anisotropy of the lock resistance to the applied force. This idea was clear to all early investigators. Lacordaire (1834) first noticed multiple teeth (fastening microtrichia) within the sutural lock in a leaf-beetle, *Chlamys*, while Heberdey (1938) demonstrated co-adaptation of hair directions in these and other fastening hairy fields. Nachtigall (1974) confirmed this observation in a diving beetle, *Cnemidotus caesus*. However, there exist no dynamometric measurements on linked elytra subjected to partition in various directions. Only Nachtigall (1974) noticed that the linked elytra resist vertically applied forces but slide apart sideways without resistance. The principle has been proven quantitatively in the insects of another order, the Heteroptera (Perez Goodwyn and Gorb, 2003). Features of natural relative partition of elytra must be taken into account when we consider disengagement or engagement of the sutural lock.

Release from the sutural lock and initial partition of the elytra are enough to notice but too small to measure against the background of broad wing spreading. The necessary angular partition of elytra is below 1°. It is not unexpected that such a tiny movement was treated only hypothetically.

Heberdey (1938) postulated that either the ventral sutural ridge of one elytron must press downwards onto the groove in the opposite elytron, in order to unclip hairy fields at the ridges, or that the opposite elytron must rise, or that both movements were simultaneous. In any case, asymmetric motion of the elytra was necessary. Even vibration of elytra was assumed. After release, elytra had to part horizontally.

Judging by the noticeable inward tilt of elytra at partition, we suggest that the axis of this initial rotation does not differ significantly from the AAA. We emphasize that unlocking the suture is caused by the simultaneous movement of both elytra. The geometry of this relative movement is described in the elytron-fixed coordinate system.

Fiori (fig. 2 in Fiori, 1975) proposed a model of co-adaptation of two symmetrical sutural profiles in opposite elytra, at the formation of the sutural lock, which obviously supported a quite different direction of locking and unlocking. According to Fiori, elytra come to engagement from below, repeating the shape of the vault. We propose that elytra part dorsad and engage from above (Fig. 14). Our suggestion is that the profile of the male component of the lock may conform to the divergence trace or divergence surface.

The strange upwardly curved profile of the male component of the lock was depicted on the very first published drawing of the sutural profile in a June cock-chafer, *Lachnosterna fusca*

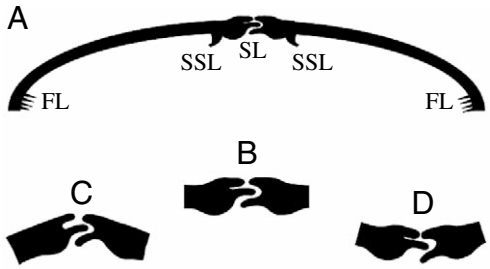

Fig. 14. Scheme of cooption of sutural ridges of two elytra in formation of the lock. (A) Transverse section across two closed elytra. Locks: FL, frictional to the metepisternum; SL, sutural clamp between elytra; SSL, subsutural click to the metanotum. (B) Parts of the sutural lock in closed elytra. (C) Direction of engagement by Fiori (1975). (D) Direction of engagement according to the present study.

(fig. 1 in Breed and Ball, 1909). Elevated dorsal ridges were also illustrated in *Hydroporus ferrugineus* (fig. 76) by Nachtigall (1974), in *Carabus morbillosus* (fig. 3), *Tenebrio molitor* (fig. 4) and the weevils *Lixus viridis* (fig. 11) and *Liparus glabrirostris* (fig. 13) by Fiori (1975), and in *Scarites buparius* (fig. 16a) by Baehr (1980).

We have seen an upwardly curved dorsal ridge only in rose-chafers (Cetoniinae), with their extremely low and backwardly oriented rotation axis. In many beetles, the curvature of the partition surface had negligible affect on the shape of the male component, whose orientation was close to the tangent to the vault of elytra. Probably, curvature of the arc of partition is not noticeable at the very short initial opening of less than 1°.

Conclusions

Complicated movement of the elytra during broad opening or closing may be quantitatively described with respect to certain reference points on the elytron. The trajectory of the apex is a flat circular arc, hence the apex rotates about the mesothorax-fixed axis. This axis comes across the elytra-to-body articulation and points contralaterad and upwards. It is tilted forward in *Melolontha hippocastani*, *Allomyrina dichotoma* and *Prionus coriarius* and backwards in *Chalcophora mariana*; in *Cetonia aurata*, the rotation axis is tilted extremely low and backwards.

Turning flatly by 90° on opening, the elytron comes to a flight position with a negative attack angle. The latter is partly compensated for by the positive pitch of the body, but even more effectively by supination of the abducting elytron about the sutural edge. Supination was demonstrated in *M. hippocastani* and *P. coriarius*. In these two species, the open elytra flap during flight across the plane of abduction–adduction. Before opening, linked elytra elevate by 10–12° about the common horizontal body-fixed axis. This movement disengages the elytron-to-body locks. At the very beginning of opening, the elytra part a little. This movement disengages the sutural lock. The axis of partition probably coincides with the axis of abduction. Reverse closing movements mimic the trajectories of opening.

By releasing the sutural lock, the elytra move relative to one

another. The trace of the relative partition is a shallow arc, convex down, opposite to the vault of linked elytra. The profile of the linking ridge in the suture in some beetles conforms to such a curved convex-down shape.

Appendix. Construction of the axis of abduction–adduction

The position of the elytron in 3-D space is defined by three points: the articulation point, O (fixed), and two arbitrary points, M and N, on the elytron. All three define the plane of the elytron. At first approximation, we suppose that the elytron rotates about a single axis. Given the initial and final position of points M and N on opening or closing (M_1, M_2 and N_1, N_2), we can find the direction of the AAA by the following construction.

(1) Construct a subsidiary plane over three points, M_1, O and M_2. Construct a bisectrix of the angle M_1OM_2, the normal to the plane M_1OM_2 at the point O, and the bisection plane over the bisectrix and the normal. All points of the bisection plane are equidistant from M_1 and M_2.

(2) Repeat the same construction for N_1, N_2.

(3) Intersection of two bisection planes is the common rotation axis. Each point in the intersection is equidistant either from M_1, M_2 or N_1, N_2, respectively. M and N rotate about this axis in parallel planes. Construction completed.

This research was partly funded by grant No 2002/90205014 from the National Natural Science Foundation of China. Qingqing Yu and Zhixian Yang took part in the flight recordings. We are indebted to Dmitry Gladun for thorough photocopying of many old articles, to Shirley Cooke who has made linguistic corrections to the manuscript and to anonymous referees, who have given many helpful suggestions.

References

Allaud, C. (1902). Note sur la conformation de la suture des élytres les Coléoptères. *Bull. Soc. Entomol.* **5**, 176-178.

Baehr, M. (1980). Zur Funktionsmorphologie und Evolutiven Bedeutung der Elytralen Sperrmechanismen der Scaritini (Coleoptera: Carabidae). *Entomol. Gen.* **6**, 311-333.

Belkaceme, T. (1991). Skelett und Muskulatur des Kopfes und Thorax von *Noterus laevis* Sturm. *Stuttgarter Beitr. Naturkunde Ser. A* **462**, 1-94.

Brackenbury, J. and Wang, R. (1995). Ballistics and visual targetting in flea-beetles, *J. Exp. Biol.* **198**, 1931-1942.

Breed, R. S. and Ball, E. F. (1909). The interlocking mechanisms which are found in connection with the elytra of Coleoptera. *Biol. Bull*. **61**, 289-303.

Brodsky, A. K. (1994). *The Evolution of the Insect Flight*. Oxford: Oxford University Press.

Fiori, G. (1975). La 'sutura' elitrale dei coleotteri. In *Atti del Congresso Nazionale Italiano di Entomologia* **10**, 91-111.

Frantsevich, L. I. (1981). The jump of the black-beetle (Coleoptera, Histeridae). *Zool. Jb. Anat.* **106**, 333-348.

Gorb, S. N. (1998). Frictional surfaces of the elytra-to-body arresting mechanism in tenebrionid beetles (Coleoptera: Tenebrionidae): design of co-opted fields of microtrichia and cuticle ultrastructure. *Int. J. Insect Morphol*. **27**, 205-225.

Haas, F. and Beutel, R. G. (2001). Wing folding and the functional morphology of the wing base in Coleoptera. *Zoology* **104**, 123-141.

Heberdey, R. F. (1938). Beiträge zum Bau des Subelytralraumes und zur Atmung der Coleopteren. *Z. Morphol. Ökol. Tiere* **33**, 667-734.

Herbst, H. G. (1944). Studien über, die Flügeldecken der Rutelinen und, Cetoniinen, (Coleoptera Scarabaeidae). Das Elytralgelenk. *Z. Morphol. Ökol. Tiere* **40**, 1-66.

Herbst, H. G. (1952). Studien über, die Flügeldecken der Rutelinen und, Cetoniinen, (Coleoptera Scarabaeidae). Das Elytralgelenk. *Zool. Jb. Anat.* **72**, 1-66.

Lacordaire, T. (1834). Introduction à l'Entomologie. *Paris* **1**, 383.

Larsén, O. (1966). On the morphology and function of locomotor organs of the Gyrinidae and other Coleoptera. *Opuscula Entomologica* **30**, 1-241.

Matsuda, R. (1970). Morphology and evolution of the insect thorax. *Mem. Entomol. Soc. Can.* **76**, 1-431.

Nachtigall, W. (1964). Zur Aerodynamik des Coleopteren-Fluges: wirken die Elytren als Tragflächen? *Verh. Dtsch. Zool. Ges*. **Suppl. 27**, 319-326.

Nachtigall, W. (1974). *Biological Mechanisms of Attachment*. Berlin: Springer.

Nikolaev, G. V. (1987). *Lamellicornian beetles (Coleoptera, Scarabaeidae) of the Kazakhstan and Middle Asia*. (In Russian.) Alma-Ata: Nauka.

Perez Goodwyn, P. J. and Gorb, S. N. (2003). Attachment forces of the hemelytra-locking mechanisms in aquatic bugs (Heteroptera: Belostomatidae). *J. Insect Physiol*. **49**, 753-764.

Pisano, P. (1982). Frequenze 'destrorsa' e 'sinistrora' del cosiddetto 'maschio' della sutura elitrale in una popolazione sarda di *Ocys harpaloides* Serv. (Coleoptera Carabidae*). Rendiconti del Seminario della Facolta di Scienze dell'Universita di Cagliari* **52**, 147-152.

Prasse, J. (1960). Über Start und Flug des *Sisyphus schaefferi* L. *Beitr. Entomol*. **10**, 168-183.

Samuelson, G. A. (1996). Binding sites: elytron-to-body meshing structures of possible significance in the higher classification of Chrysomeloidea. In *Chrysomelidae Biology: The Classification, Phylogeny and Genetics*, vol. 1 (ed. P. H. A. Jolivet and M. L. Cox), pp. 267-290. Amsterdam, The Netherlands: SPB Academic Publishing.

Schneider, P. (1978). Die Flug- und Faltungstypen der Käfer (Coleoptera). *Zool. Jb. Anat.* **99**, 174-210.

Schneider, P. (1986). Studies about the flight of *Dytiscus marginalis*. 1. (Coleoptera, Dytiscidae). *Entomologica Basiliensia* **11**, 451-460.

Schneider, P. (1987). Mechanik des Auf- und Abschlages der Hinterflügel bei Käfern (Coleoptera). *Zool. Anzeiger* **218**, 25-32.

Schneider, P. and Hermes, M. (1976). Die Bedeutung der Elytren bei Vertretern des Melolontha-Flugtyps (Coleoptera). *J. Comp. Physiol*. **106**, 39-49.

Schneider, P. and Krämer, B. (1974). Die Steuerung des Fluges beim Sandlaufkäfer (*Cicindela*) und beim Maikäfer (*Melolontha*). *J. Comp. Physiol*. **91**, 377-386.

Schneider, P. and Meurer, J. (1975). Die mittelbar-indirekte Bewegung der Elytren beim Nashornkäfer *Oryctes boas* Fabr. (Coleoptera). *Zool. Jb. Physiol*. **79**, 297-310.

Stellwaag, F. (1914). Der Flugapparat der Lamellicornier. *Z. Wiss. Zool.* **108**, 359-429.

Straus-Duerkheim, H. E. (1828). Considérations générales sur l'anatomie comparée des animaux articulees. Paris.